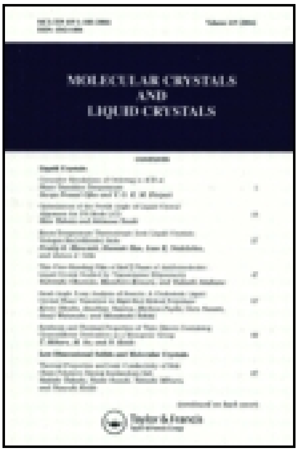

Molecular Crystals and Liquid Crystals
Publication details, including instructions for authors and subscription information:
http://www.tandfonline.com/loi/gmcl20

Fast Humidity Sensing and Switching of $LiNbO_3$ Films on Silicon

Svetlana Bravina [a], Nicolas Morozovsky [a], Elhadj Dogheche [b] & Denis Remiens [b]

[a] Institute of Physics NASU, Kyiv, Ukraine

[b] IEMN-DOAE-MIMM Team, Villeneuve d'Ascq, France

Version of record first published: 03 Mar 2011

To cite this article: Svetlana Bravina, Nicolas Morozovsky, Elhadj Dogheche & Denis Remiens (2011): Fast Humidity Sensing and Switching of $LiNbO_3$ Films on Silicon, Molecular Crystals and Liquid Crystals, 535:1, 196-203

To link to this article: http://dx.doi.org/10.1080/15421406.2011.538341

Mol. Cryst. Liq. Cryst., Vol. 535: pp. 196–203, 2011

ISSN: 1542-1406 print/1563-5287 online
DOI: 10.1080/15421406.2011.538341

Fast Humidity Sensing and Switching of $LiNbO_3$ Films on Silicon

SVETLANA BRAVINA,[1] NICOLAS MOROZOVSKY,[1] ELHADJ DOGHECHE,[2] AND DENIS REMIENS[2]

[1]Institute of Physics NASU, Kyiv, Ukraine
[2]IEMN-DOAE-MIMM Team, Villeneuve d'Ascq, France

The influence of a pulse humidity impact on the electrophysical parameters of Pt/$LiNbO_3$-film/Pt:Ti/SiO_2/Si structures is investigated. A continuous transformation of the current-voltage, charge-voltage, and transient characteristics with the reaction time ~1 s and the recovery time ~10 s (under a low humidity impact), as well as a transformation of the threshold switching type (under a high humidity impact), are observed. The peculiarities of current-voltage loops and transient currents correspond to the relay-race charge transfer.

The efficiency of dynamic methods for studying the influence of fast humidity changes on the electrophysical characteristics of $LiNbO_3$ films is demonstrated, and the possible applications to high-speed humidity sensing are considered.

Keywords Dynamic electrophysical characterization; fast humidity sensing; lithium niobate films

1. Introduction

The applications of $LiNbO_3$ (LN) single crystals are well known for nonlinear optics, acousto-electronics, and infrared sensorics. The modern trend in integrated nonlinear optics and optoelectronics includes a successive replacement of LN thin plate functional elements with LN-film on silicon substrate (LN-film/Si) structures that can be considered as promising for designing various elements of Si-based functional optoelectronics.

The LN-film/Si structures are considered as promising for replacement LN thin plate single crystalline elements of functional optoelectronics, in particular for surface acoustic wave (SAW) devices, non-linear optics (wave-guides and frequency doublers), and telecommunication (optical switchers and filters) applications [1, 2]. The structures of LN-film/Si are also attractive for integrated ferroelectric random access memories (FeRAM) [3].

The environment monitoring demands the development of sensitive and high-speed humidity sensors integrated in a modern Si-base. Recently, we have investigated the dynamic humidity-electric activity of surface-active zeolite-like systems and mesoporous phases [4], some of porous ceramics [5], and porous silicon [6, 7].

Address correspondence to Svetlana Bravina, Institute of Physics NASU, 46, Prospect Nauky, Kyiv 03028, Ukraine. E-mail: bravina@iop.kiev.ua

An apparent humidity influence on the surface conductivity of LN single crystals was also reported [8].

In view of the stable tendency of integrating functional elements including ferroelectric-based structures into Si-based environment microelectronics that operate not only in a static mode but also in a dynamic one, it is reasonable to perform the dynamic characterization for LN-film/Si structures as surface-active systems. On the other hand, due to the criticality of a humidity level for the operation of electronic components, the investigations of the humidity impact on the electrophysical characteristics of an LN-film in the pulse mode under environmental conditions similar to ones of operating Si-based devices are desirable.

In this paper, we present the results of investigations of dynamic current-voltage and charge-voltage loops and transient currents under the pulse humidity impact for LN-film/Si structures.

2. Experimental

2.1. *Samples*

In Pt/$LiNbO_3$-film/Pt:Ti/SiO_2/Si-substrate structures, LN-films were prepared by the radio-frequency magnetron sputtering technique on a Pt-covered Si-substrate. The deposition procedure and the X-ray diffraction structure analysis are similar to those for LN/Al_2O_3 structures described previously [2].

The sputtering target was a cold-pressed pellet 75 mm in diameter made of commercial $LiNbO_3$ powder. The optimal growth temperature was selected 490–500°C for obtaining the films of a single-phase composition with minimal Li deficiency. The thickness of the obtained LN-film was 0.4–1.1 μm depending on the corresponding deposition time 4–11 h. By the AFM surface mapping, the average surface roughness from 5 to 15 nm depending on the film thickness was revealed.

The bottom Pt/Ti-bilayer was deposited onto the oxidized (350 nm of SiO_2) (100) *n*-type Si substrate 350 μm in thickness. The top Pt-electrodes 0.15 mm^2 in area were deposited by the sputtering procedure which was followed by a lift-off.

As a comparative model material for examining the phenomena connected with a complex-type conductivity, the samples of semiconductor-ionic crystal proustite, Ag_3AsS_3, with mixed Ag-ion-electronic electrical conduction [9, 10] were used. The Ag_3AsS_3 samples were prepared from single crystal polished *Z*-cut plates 0.5–0.8 mm in thickness and 3–10 mm^2 in area with vacuum evaporated Au-electrodes.

2.2. *Measurements*

We investigated the variations of parameters of dynamic current-voltage (*I*-*V*-) and charge-voltage (*Q*-*V*-) loops and the dynamic transient currents (*I*-*t*-curves) induced by a humid air pulse 1–5 sec in duration.

Under studying the *I*-*V*-loops and the *I*-*t*-curves, the series reference resistor was used, and, during the studies of the *Q*-*V*-loops, the series reference capacitor was used, the same as under investigations of the corresponding characteristics of ferroelectric capacitors [11]. The measurements were performed in the multicycle mode under an applied a.c. triangular drive voltage (for *I*-*V*- and *Q*-*V*-loops) and a meander voltage (for *I*-*t*-curves) in the frequency range 1 Hz – 1 kHz and the voltage range 10 mV – 10 V.

The change of sample parameters under an applied voltage and/or a relative humidity H_r variation can be characterized by a change of parameters of the equivalent series-parallel resistive-capacitance (R-C-) circuit with pronounced $R(V)$ and $C(V)$ dependences [7, 10].

The main peculiarities of I-V-loops can be considered using a simplified parallel R-C-circuit neglecting the effect of the series resistor and the capacitor. Since, for this R-C-circuit, $I(V) = d(CV)/dt + V/R$, under $V = V_0(1 \pm bt)$ with b =const and C = const, the current value is $I(V) = I(V_0, t) = V_0[\pm bC + (1/R)(1 \pm bt)]$.

The increase (decrease) of the slope and the vertical size of an I-V-loop indicates a simultaneous increase (decrease) of $1/R$ and C values. At that, dI/dV value and $\pm bC$ range under $V = 0$ reflect zero voltage $1/R_0$ and C_0 values, respectively. Generally, analyzing the deviation of $I(V)$ from linearity gives the information concerning $R(V)$ and $C(V)$ dependences.

The temporal changes of the investigated characteristics of the examined structures during and just after a humid air pulse and under restoration of the initial state were also registered.

3. Results and Comments

3.1. *Low Drive Voltage Values*

Figure 1 presents I-V- and Q-V-loops before and after the humid air pulse impact under relatively low drive voltage values. The shape of the low-voltage parts of I-V-loops at low H_r values corresponds to a linear equivalent series-parallel R-C-circuit. The observed transformations, in particular an increase of the slope of I-V-loops and the vertical size of I-V- and Q-V-loops under an increase of H_r, correspond to a simultaneous decrease of R and an increase of C together with increase of R- and C- voltage nonlinearities. The observed increase of the vertical size of Q-V-loops corresponds to an increase of the value of transferred electrical charge. The relative changes of C and R (Fig. 1a) and Q (Fig. 1b) under a humid air pulse are about 6, 20, and 30 times, respectively.

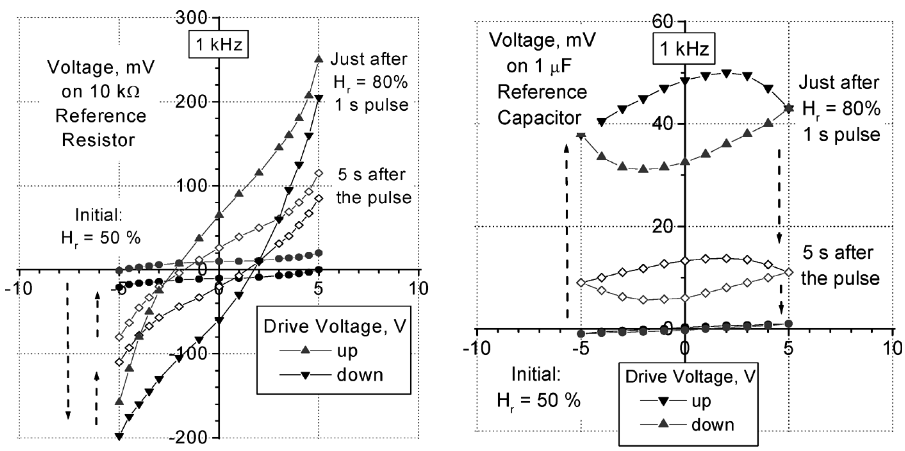

(a) (b)

Figure 1. Dynamic current-voltage loops (a) and charge-voltage loops (b) of $Pt/LiNbO_3/Pt{:}Ti/SiO_2/Si$ structure (1 kHz) before and after the impact of a humid air pulse.

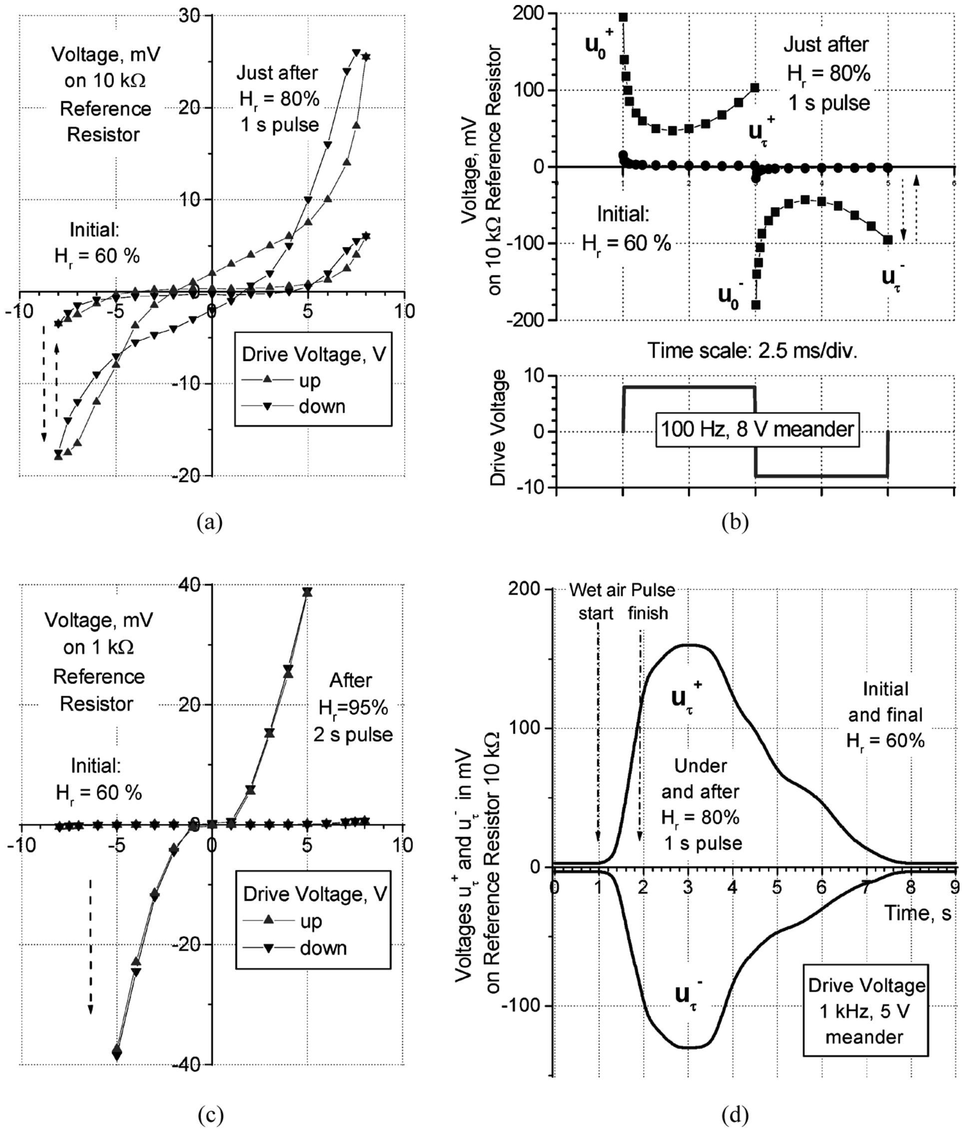

Figure 2. Current-voltage loops (10-Hz drive voltage) (a), transient currents (100-Hz drive voltage) (b) at a low-humidity impact and current-voltage loops at a high-humidity impact (c), and the traces of characteristic voltages U_τ^+ and U_τ^- of dynamic transient current curves (d) for Pt/LiNbO$_3$/Pt:Ti/SiO$_2$/Si structure before, under, and after the humid air pulse impact.

The observed *I-V*-loops asymmetry noticeable in Figure 1*a* is apparently a consequence of different microstructure states of LN-film under Pt-top and Pt:Ti-bottom electrodes. This asymmetry leads to the rectification effect which is the reason of the predominance of the charge of definite sign in the charge transfer during every period of a.c. driving voltage change. As a result, the vertical shift of *Q-V*-loops (the so-called imprint) takes place.

The forward transformation (under H_r rise) and the reverse one (to the initial state under subsequent drying) (see the dashed arrows in Fig. 1*a,b*) occurs during $\tau_f \approx 1$–2 s and $\tau_r \approx 5$–10 s, respectively, depending on the humid air pulse duration.

3.2. *High Drive Voltage Values*

Figure 2 presents *I*-*V*-loops and *I*-*t*-curves before and after humid air pulse impact under relatively high drive voltage values. The degree of *I*-*V*-loop non-linearity is frequency- and voltage-dependent. At infra-low frequencies (~10 Hz), the *I*-*V*-loops show a high degree of voltage *R*- and *C*-non-linearity and a well-pronounced humidity-dependent hysteretic behavior (Fig. 2*a*). Increasing H_r leads to broadening the hysteresis regions of *I*-*V*-loops.

The transformation of an *I*-*t*-curve consists in a significant increase of the initial voltages U_0^+ and U_0^- at the time moment of the meander pulse start and the final ones U_τ^+ and U_τ^-, which corresponds to the end of a meander pulse. The appearance of the minima on *I*-*t*-curves and so the transition from decreasing to increasing $I(t)$ (Fig. 2*b*) correlates with the hysteretic behavior of *I*-*V*-loops.

Under a short-term high humidity impact, the transformation of *I*-*V*-loops to the view characteristic of the threshold switching to a high-conduction state was observed (Fig. 2*c*). The time of switching is ~0.1 s. The initial low-conduction state is achieved after a drive voltage getting off. So, the reversible bistable humidity-driven switching is possible. A long-term high-humidity impact leads to the irreversible breakdown of a film.

Figure 2*d* presents changes of U_τ^+ and U_τ^- under and just after the humidity pulse impact. The traces of voltages U_τ^+ and U_τ^- obtained during a humid air pulse and under restoration of the initial state demonstrate a difference in the reaction time on the impact of a humid air pulse (~1 s) and the restoration time (≈ 5 s). Non-uniformities noticeable on U_τ^+ and U_τ^- drops are connected with the non-constant rate of absorbate evaporation.

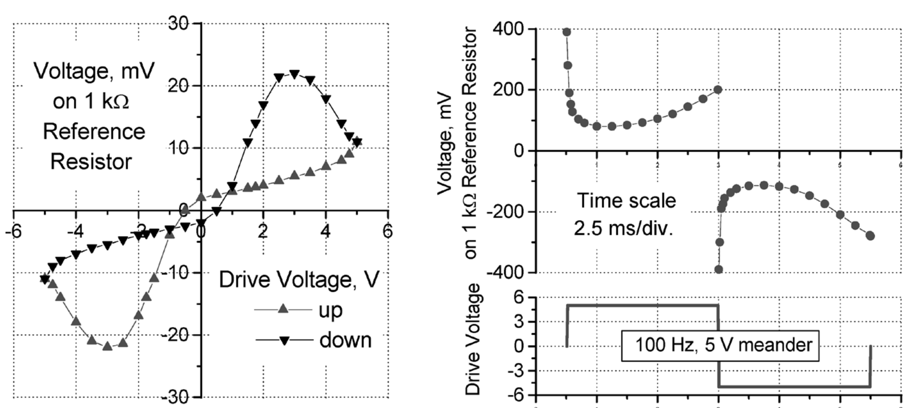

(a) (b)

Figure 3. Current-voltage loop (10-Hz drive voltage) (a) and transient currents (100-Hz drive voltage) (b) for the Au-Ag_3AsS_3-Au structure under normal conditions.

3.3. *Comparison with Semiconductor-Ionic Characteristics*

Figure 3 presents *I-V*-loops and *I-t*-curves for a semiconductor-ionic Ag_3AsS_3 sample. The specific propeller-like shape of *I-V*-loops (Fig. 3*a*) and minima on *I-t*-curves (Fig. 3*b*) are connected with the mixed Ag^+-e^- charge transport inherent to Ag_3AsS_3–family crystals, of which the formation of the ionic space charge in the under-surface region is characteristic [9, 10].

The shape and the trace direction of *I-V*-loops for Ag_3AsS_3 are similar to those observed for LN-film/Si structures under the H_r variation (compare Fig. 2*a* and Fig. 3*a*). The similar shape of *I-t*-curves (compare Fig. 2*b* and Fig. 3*b*) reflects similar features of the time behavior for Ag_3AsS_3 exposed to an electric field and LN-film/Si structures exposed to a humid air pulse.

The increasing relaxation on *I-t*-curves for LN-film/Si is similar to that observed for the model semiconductor-ionic Ag_3AsS_3 and Ag_3SbS_3, for which the relay-race charge transfer [12] was established [9, 10], and the electrolytic-type reaction $Ag_{Ag} + e^- = V^-_{Ag} + Ag^+ + e^- = V^-_{Ag} + Ag^0$ takes place in the near-electrode subsurface layer. The indicated similarity of *I-V*-loops and *I-t*-curves observed for LN-film/Si and those observed for the model semiconductor-ionic Ag_3AsS_3 points to an apparent contribution of ionic transfer processes.

4. Discussion

The change of the shapes of *I-V*-loops and *I-t*-curves under an H_r variation can be characterized by a linear parallel *R-C*-circuit for its low-voltage parts and by a series-parallel circuit with pronounced $R(V)$ and $C(V)$ non-linearities of all the components for their high-voltage parts.

The observed transformations of *Q-V*- and *I-V*- loops are in good correspondence. In particular, the vertical shift of *Q-V*-loops is connected with the rectification effect as a consequence of the *I-V*-loops asymmetry, which leads to the accumulation of d.c. electric charge on the reference capacitor during every period of the a.c. driving voltage change.

The data obtained for LN-film systems prove the great influence of the processes of absorption and dissociation of polar H_2O molecules due to the surface activity of structures. Moreover, we have demonstrated the possibility of not only continuous Q-V- and I-V- loops transformations (under a short-term low-humidity impact), but also a transformation of the threshold switching type (under a short-term high-humidity impact) up to the film breakdown (under a long-term high-humidity impact).

For the investigated LN-film/Si-structures, the observed peculiarities of *Q-V*- and *I-V*- loops and *I-t*-curves are connected with the adsorption of H_2O vapor, post-dissociation of water molecules ($H_2^+O^{2-} \rightarrow H^+ + OH^-$), and ion-electronic ($H^+$, e^- or OH^-) relay-race charge transfer [12] through the volume of an LN-film and the subsequent desorption of H_2O as a temporal source of ionic charge carriers.

The observed changes of *I-V*- and *Q-V*- loops parameters of LN-film/Si structures under a humid air pulse impact are similar to those of porous Si/Si structures [6, 7]. So we can assume that the LN-film/Si structures under investigation possess some degree of porosity.

The mechanism of charge transfer in porous Si is connected with the hopping transport by means of switching the dangling bonds [14]. The kinetics of these processes determines shapes of the corresponding characteristics and peculiarities of their time behavior.

The results obtained for the samples of porous Si/Si [6, 7] are comparable with those obtained for zeolite-like (of Na-Y type) and silica mesoporous systems (of MCM-41 type) [4] and porous metal-oxide ceramics [5]. These systems can be considered as relatively inertial media for reactions connected with the dissociation of water molecules. In the case of LN-films, the processes with participation of the O^{2-}-sublattice (by oxygen vacancies) and the Li^+-sublattice (by Li^+-cations and/or V_{Li}^--vacancies and by the H_{Li}^+ hopping) should be considered. As a consequence of the Li-O_{H_2O} interaction and the donor-acceptor character of Li-O bonds, the configuration of an H_2O molecule is approaching that of the H-O-H group [15].

The high-speed response on a humidity impact (see 3.1 and 3.3) can be connected with the H^+-transfer at the boundary of the water adsorbate and the porous mixed oxide adsorbent, where the conditions of the so-called synchronous transport [15] can be realized through H_{Li}^+-chains.

The observed time scale of the transformation of *I*-*V*-loops (as well as *I*-*t*-curves and *Q*-*V*-loops) under a humidity impact in the sequence "change of the shape – stabilization in time – shape restoration" with a certain degree of approximation can be considered as that corresponding to characteristic times in the sequence "adsorption – transfer – desorption".

5. Application Aspect

The reaction of resistance *R* and capacitance *C* on the humidity change is well registered by means of a transformer *RC*-bridge with oscilloscopic indication.

For monitoring the humidity variations, the *R*- or *C*- changes of a humidity sensitive element can be converted into a frequency-timing code by its insertion into the corresponding frequency control circuit of an *RC*- or *LC*- generator [5]. The direct conversion of humidity changes to the frequency-time code was realized by using an *RC*-generator based on an amplifier with dynamic load [16] or an operational amplifier with feed-back circuits. The connection of a humidity sensitive element to the radio frequency resonance *LC*-bridge with sound frequency output at the beat frequency between the frequencies of the reference and "humidity sensitive" *LC*-circuits gives a siren-like response on the humidity pulse.

6. Conclusion

For $LiNbO_3$-film/Si structures as an example of surface-active systems, we have shown the efficiency of using the methods of dynamic electrophysical characterization for studying the changes of characteristics of these materials under fast humidity changes.

The view of the current-voltage and transient current-time curves under and after the humidity pulse impact is characteristic of the poling processes in the space charge region similar to those observed in typical semiconductor-ionic materials under high enough voltage application.

The transformation of current-voltage loops from the reversible continuous (under low-humidity impacts) up to the threshold switching type (under short-term high-humidity impacts) in $LiNbO_3$-film/Si structures gives a possibility of considering the ferroelectric film/Si systems as promising for fast humidity sensors of various types, in particular, humidity-switched sensors for high-speed humidity controlling devices of monitoring systems.

The observed humidity impact should be taken into account under operation with non-evacuated film structures based on non-ferroelectric and polar-active ferroelectric-like surface-active materials.

Acknowledgment

The work was supported by the Ministry of Education and Science of France, Conseil Regional Nord-Pas-de-Calais and the University of Valenciennes.

References

[1] Choi, C. W., Kwon, Y.- U., & Lee, J. (1998). *J. Korean Phys. Soc.*, *32*, S1417.
[2] Lansiaux, X., Dogheche, E., Remiens, D., Guilloux-viry, M., Perrin, A., & Ruterana, P. (2001). *J. Appl. Phys.*, *90*, 5274.
[3] Kim, K.- H., Lee, S.- W., Lyu, J.- S., Kim, B.- W., & Yoo, H.- J. (1998). *J. Korean Phys. Soc.*, *32*, S1417.
[4] Bravina, S. L., Morozovsky, N. V., Tel'biz, G. M., & Shvets, A. V. (1999). Materials of International Conference on Optical Diagnostics Materials and Devices for Opto-, Micro and Quantum Electronics, SPIE: Kiev, 95.
[5] Bravina, S. L., Morozovsky, N. V., & Khaikina, E. G. (2000). Materials of 12th IEEE International Symposium on the Application of Ferroelectrics (ISAF), Hawaii, 121.
[6] Bravina, S. L., & Morozovsky, N. V. (2002). Materials of Second Open French-Ukrainian Meeting on Ferroelectricity and Ferroelectric Thin Films, Dinard, 125.
[7] Bravina, S. L., Morozovsky, N. V., & Boukherroub, R. (2006). *Semiconductor Phys. Quantum Electron. & Optoelectronics*, *9*, 79.
[8] Maeda, M., Suzuki, I., & Jakiyama, K. (1992). *Jpn. J. Appl. Phys.*, *31*, 3229.
[9] Morozovsky, N. V. (1981). *Phys. and Techn. of Semicond.*, *15*, 2396.
[10] Bravina, S. L., & Morozovsky, N. V. (1983). *Phys. and Techn. of Semicond.*, *17*, 824.
[11] Burfoot, J. C., & Taylor, G. W. (1979). *Polar Dielectrics and Their Applications*. Macmillan: London.
[12] Timan, B. L. (1973). *Phys. and Techn. of Semicond.*, *7*, 225.
[13] Foucaran, A., Sorli, B., Garcia, M., Pascal-Delannoy, F., Giani, A., & Boyer, A. (2000). *Sens. Actuators A*, *79*, 189.
[14] Stievenard, D., & Deresmes, D. (1995). *Appl. Phys. Lett.*, *67*, 1570.
[15] Sokolov, N. D. (1955). Uspekhi Fiz. Nauk, *57*, 205.
[16] Bravina, S. L., Vysochansky, Yu. M., Kremenchugsky, L. S., Morozovsky, N. V., & Slivka, V. Yu. (1988). *Patent N1471817 USSR, MKI GO1 K 7/32*.